[redacted]

NATIONAL ADVISORY COMMITTEE FOR AERONAUTICS

TECHNICAL NOTE 1985

ELASTIC BUCKLING OF OUTSTANDING FLANGES CLAMPED AT ONE EDGE AND REINFORCED BY BULBS AT OTHER EDGE

By Stanley Goodman

National Bureau of Standards

Washington
October 1949

NATIONAL ADVISORY COMMITTEE FOR AERONAUTICS

TECHNICAL NOTE 1985

ELASTIC BUCKLING OF OUTSTANDING FLANGES CLAMPED AT ONE EDGE AND REINFORCED BY BULBS AT OTHER EDGE

By Stanley Goodman

SUMMARY

The compressive buckling stress of outstanding flanges reinforced by bulbs was computed by the strain-energy method for flanges having 10 shapes and a range of lengths. The results were checked for some cases by computations based on a differential-equation method. The edge of the flange opposite the bulb was considered clamped, and the loaded ends were considered simply supported. The results were analyzed to determine which shape of flange gave the greatest support to the structure to which it was attached. It was found that the flange capable of giving the most support without buckling had an over-all flange width of $3.4\sqrt{A_F}$ (where A_F is the cross-sectional area of the flange). This flange was somewhat slimmer than the one previously found best for the case of a simply supported flange root.

INTRODUCTION

Flanges reinforced by bulbs are widely used to reinforce the stressed skin in semimonocoque aircraft structures. They perform a two-fold function in the structure by (1) maintaining the structural shape and (2) carrying a substantial portion of the externally applied load.

The outstanding flanges in such structures have a tendency to fail under compressive load by a lateral displacement of the outstanding portions of the flange with respect to the rest of the structure. As is pointed out in reference 1, such a failure is intermediate between torsional instability in which no cross-sectional distortion of the flange occurs (considered by Goodier in reference 2, Kappus in reference 3, and Lundquist and Fligg in reference 4) and local instability of component elements of the structure in which the lines joining component plates remain straight (considered by Timoshenko in reference 5, Kroll in reference 6, and Lundquist, Stowell, and Schuette in reference 7).

The lateral instability of outstanding flanges under compressive load, for the case where the flange has a reinforcing bulb at its outer edge, has received considerable study. Windenburg (reference 8) considered both local and primary instability of flanges having a reinforcing bulb symmetrically placed on both sides of the flange web. He considered the case of simple support of the flange by the structure to which it is attached. Chwalla (reference 9) considered the case where the structure gives clamped support to the flange and presented numerical results for certain specific cases.

A survey (reference 1) of aluminum-alloy extrusions showed that the shape of most reinforcing bulbs is either rectangular with a rounded end and a fillet at the junction of the bulb and flange or circular with a fillet at the junction of the bulb and the flange. In nearly all cases the bulb was entirely on one side of the flange, thus resulting in an unsymmetrical distribution of material at the outer edge of the flange. It was found that the range of cross-sectional shapes used could be approximately covered by 54 specific flange shapes.

In reference 1, numerical solutions were given in dimensionless form for the lateral instability of these 54 different flanges as a function of the flange length. The edge condition along the line of attachment to the structure was taken as the extreme of simple support. In the present paper, the case of clamped support will be treated and, of the 54 cross sections analyzed in reference 1, only a representative group of 10 will be considered.

This work was conducted at the National Bureau of Standards under the sponsorship and with the financial assistance of the National Advisory Committee for Aeronautics.

SYMBOLS

A_b	cross-sectional area of bulb; bulb includes area cross-hatched in figure 1
A_F	cross-sectional area of flange
A_s	cross-sectional area of sheet in sheet-stringer structure
b	flange width from base to bulb center
b_1	width of rectangular-type bulb from free end to center line of web

D	flexural rigidity of web $\left(\frac{Et^3}{12(1-\nu^2)}\right)$
E	Young's modulus
G	shear modulus $\left(\frac{E}{2(1+\nu)}\right)$
ν	Poisson's ratio; 0.3
I	moment of inertia
I_b	moment of inertia of bulb about center line of web
I_F	moment of inertia of flange about its base
J_T	torsion constant of bulb
L	flange length
t	flange thickness
t_1	thickness of rectangular-type bulb
R	fillet radius of rectangular-type bulb, taken equal to t_1
R_1	fillet radius of circular-type bulb
R_2	bulb radius of circular-type bulb
w	lateral displacement of flange
σ_x	compressive end stress
σ_{cr}	critical stress for instability of flange
σ_{cr_s}	critical stress for sheet-stringer structure
$\sigma_{cr_{min}}$	critical stress for instability of an infinitely long flange
φ	angle of twist of bulb with respect to web
x	coordinate along flange length
y	coordinate along flange width

SHAPE OF REINFORCED FLANGES

The shapes of the reinforced flanges are shown in figure 1 and their properties and dimensions are given in table 1. Five of the flanges had essentially rectangular reinforcing bulbs, while, for the remaining five, the bulbs were essentially circular. The first column in table 1 gives the flange number. The second column gives the number of the corresponding flange considered in reference 1. The third column gives the thickness of the flange web, and columns (4) to (6) give dimensionless ratios describing the shape of the cross section.

ANALYSIS

The flanges considered in this report are clamped at the root edge and get lateral and torsional support at the outer edge from the reinforcing bulb. For such a flange, no bending is possible in the plane of the web and, therefore, any bending which does occur will have the web center line as a neutral axis. This fact will allow a conventional treatment for the unsymmetrical reinforcing bulbs (fig. 1) considered in this report. The buckling stress of the flange will be computed as that of a plate clamped at one edge and restrained at the other edge by a beam. This beam will have a bending stiffness EI_b equal to that of the cross-hatched area of figure 1 about the center line of the web, a torsional stiffness GJ_T equal to that of the whole flange (fig. 1) less that of the web, and an area A_b equal to that of the cross-hatched area of figure 1. Values of I_b, J_T, and A_b are given in columns (7), (8), and (9) of table 1. The total area of the flange A_F is given in column (10) of table 1. The flexural rigidity D is given as D/E in column (11) of table 1.

Plate Theory

An expression for the compressive buckling stress was first obtained by integrating the differential equation of the deflection surface to find the magnitude of the compressive stress necessary to keep the plate in a slightly buckled shape. The derivation of this method appears in the appendix. Since the integration method appeared excessively cumbersome, a strain-energy method was developed, using the technique given on pages 325 to 327 of reference 5 as follows:

The work of the external forces on the plate and beam (see p. 325, reference 5) is

$$(1/2)\int_0^b\int_0^L \sigma_x t\left(\frac{\partial w}{\partial x}\right)^2 dx\,dy + \frac{\sigma_x A_b}{2}\int_0^L \left(\frac{\partial w}{\partial x}\right)^2_{y=b} dx = I_2\sigma_x \qquad (1)$$

The strain energy of the beam and plate, neglecting shear in the beam is (see pp. 325, 24, and 265, reference 5)

$$(D/2)\int_0^b\int_0^L \left\{\left(\frac{\partial^2 w}{\partial x^2}+\frac{\partial^2 w}{\partial y^2}\right)^2 - 2(1-\nu)\left[\frac{\partial^2 w}{\partial x^2}\frac{\partial^2 w}{\partial y^2}-\left(\frac{\partial^2 w}{\partial x\partial y}\right)^2\right]\right\} dx\,dy +$$

$$\frac{EI_b}{2}\int_0^L \left(\frac{\partial^2 w}{\partial x^2}\right)^2_{y=b} dx + \frac{GJ_T}{2}\int_0^L \left(\frac{d\varphi}{dx}\right)^2_{y=b} dx = I_1 \qquad (2)$$

where

$$\varphi = \left(\frac{\partial w}{\partial y}\right)_{y=b} \qquad (3)$$

In order to obtain the results in dimensionless form it was convenient to set $\nu = 0.3$, $G = E/2.6$ and to work with I_1', defined by

$$I_1' = I_1/E = (D/2E)\int_0^b\int_0^L \left\{\left(\frac{\partial^2 w}{\partial x^2}+\frac{\partial^2 w}{\partial y^2}\right)^2 - 1.4\left[\frac{\partial^2 w}{\partial x^2}\frac{\partial^2 w}{\partial y^2}-\left(\frac{\partial^2 w}{\partial x\partial y}\right)^2\right]\right\} dx\,dy +$$

$$\frac{I_b}{2}\int_0^L \left(\frac{\partial^2 w}{\partial x^2}\right)^2_{y=b} dx + \frac{J_T}{5.2}\int_0^L \left(\frac{d\varphi}{dx}\right)^2_{y=b} dx \qquad (4)$$

A function allowing a single buckle in the x-direction,

$$w = \left(\sin\frac{\pi x}{L}\right)\left(a_1y^2 + a_2y^3 + a_3y^4 \ldots a_ny^{n+1}\right) \qquad (5)$$

where a_1, a_2, . . ., a_n are arbitrary constants, was chosen to represent the deflection surface of the plate.

The critical stress is given by the expression (reference 5, p. 326)

$$I_2\sigma_{cr} = I_1 \tag{6}$$

or, using equation (4),

$$\sigma_{cr}/E = \frac{I_1'}{I_2} \tag{7}$$

The values of the constants a_1, a_2, . . . in equation (5) are determined from the condition that they give the lowest possible buckling stress σ_{cr}. For this to be true they must satisfy the set of simultaneous equations (reference 5, p. 326)

$$\left.\begin{aligned} \frac{\partial I_1'}{\partial a_1} + \frac{\sigma_{cr}}{E}\frac{\partial I_2}{\partial a_1} = 0 \\ \frac{\partial I_1'}{\partial a_2} + \frac{\sigma_{cr}}{E}\frac{\partial I_2}{\partial a_2} = 0 \\ \cdot \quad \cdot \quad \cdot \quad \cdot \quad \cdot \end{aligned}\right\} \tag{8}$$

Solutions of equations (8) different from zero may be obtained only if the determinant of the equations is zero.

The expressions for I_1' and I_2 may be obtained by substituting equation (5) in equations (4) and (1), respectively. The critical buckling stress may then be obtained by substituting the expressions obtained for I_1' and I_2 in equation (8), setting the determinant of the resulting equations equal to zero, and solving for the lowest values of σ_{cr}/E.

Convergence

To determine the minimum number of arbitrary constants necessary in equation (5) for accurate determination of the buckling stress, the buckling-stress ratio of flange 5 with $L/\sqrt{A_F} = 5.396$ was computed three times, using one, two, and three arbitrary constants in equation (5), successively. The buckling-stress values according to the strain-energy method were as follows:

Number of arbitrary constants in deflection equation	Values of σ_{cr}/E obtained
1	0.0308
2	.0282
3	.0233

The convergence seemed slow. To obtain additional information on this point, the buckling stress was also computed by the integration method with the result $\sigma_{cr}/E = 0.0233$.

It was concluded that in this case the equation

$$w = \left(\sin \frac{\pi x}{L}\right)\left(a_1 y^2 + a_2 y^3 + a_3 y^4\right) \tag{9}$$

has the minimum number of arbitrary constants necessary to adequately represent the deflection surface.

Buckling stress-ratio values for one or more length-ratio values were computed for each of the 10 flange shapes by the integration method given in the appendix for comparison with the corresponding buckling stress obtained by the strain-energy method using equation (9). Stress-ratio values obtained by both methods are given in table 2. In all cases the results of the two methods agree within the accuracy of the numerical computations. It was concluded that equation (9) would be sufficiently accurate and the remaining computations were done by the strain-energy method using equation (9).

Contribution of Bulb to Critical Stress

The contributions of the bending stiffness and torsional stiffness, respectively, to the buckling stress of flange 4 at $L/\sqrt{A_F} = 18.91$ were determined by recomputing the buckling stress ratio twice, first omitting the bending-stiffness term, and then omitting the torsional-rigidity term. It was found that omission of the bending-stiffness term reduced the buckling stress-ratio value from 0.0147 to 0.0086, or 41 percent, and that omission of the torsional-stiffness term reduced it from 0.0147 to 0.0134, or only 9 percent.

Multiple Roots

In the strain-energy method, the critical stress is found from the condition that the determinant of the coefficients of three simultaneous equations shall be zero. This determinant, when expanded, is a cubic

equation, and as a result more than one solution is possible. In order to make sure that the solution obtained was that corresponding to the lowest buckling load, a plot was made, in some cases, of the value of the determinant as a function of the assumed critical stress, starting from zero stress. The first intersection with the zero axis was taken as the lowest critical stress. This method was used only in those cases where there was some doubt as to whether the stress obtained actually corresponded to the lowest critical stress. In the other cases, values of the determinant were obtained only in the neighborhood of the estimated zero point.

RESULTS

Critical Stress

The buckling stress ratio σ_{cr}/E is plotted in figure 2 against the length ratio $L/\sqrt{A_F}$ for the 10 flange shapes considered. The ratio $L/\sqrt{A_F}$ was chosen as the abscissa since it has a fixed value for all geometrically similar specimens and it also has a fixed value for all geometrically different specimens of a given length having the same cross-sectional area. Comparison of ordinates for a given abscissa will therefore show the effect of changing the distribution of material in the flange.

The buckling stress ratios in figure 2 decrease rapidly with increasing flange length, go through a minimum at a flange length lower than that usually encountered in aircraft structures, and rise rapidly for greater flange lengths. Stubby flanges are more stable than wide, thin flanges, and, except in the case of the two narrowest flanges, flanges reinforced by rectangular bulbs are more stable than those reinforced by round bulbs.

Flanges as long as those commonly used in aircraft structures will buckle longitudinally into a number of half sine waves. In the case of flanges with simply supported loaded ends the number of half waves into which the flange buckles and the buckling stress for any length may be obtained by plotting a family of curves, using the ordinates of the original stress-ratio, length-ratio curve, and multiples 1, 2, 3, and so forth of the corresponding abscissas, successively, as in figure 3. The transition from a buckle pattern of one half wave to that of two half waves occurs at the intersection of the first and second curves so drawn, from two to three half waves at the intersection of the second and third curves, and so forth. The critical stress ratio for any length ratio may be obtained from the curve having the lowest ordinate at that length ratio. With increasing length ratio the buckling stress

ratio approaches a constant minimum value $\sigma_{cr_{min}}/E$. Deviations from this minimum value are generally small in the range of flange lengths $L > 20\sqrt{A_F}$.

Transverse Deflections of Web Center Line

An expression for the relative transverse deflection of the web center line of each of six flanges subjected to buckling stress was obtained as follows: Two of equations (8) were arbitrarily selected and the buckling stress ratio was substituted for σ_{cr}/E. The coefficient a_3 was then factored out and the resulting equations were solved simultaneously for a_1/a_3 and a_2/a_3. Using equation (9), the relative values of the deflections were computed.

These deflections are plotted in figure 4, for three flanges with rectangular bulbs, and in figure 5, for three flanges with circular bulbs. In figures 4 and 5, the ordinate is the ratio of the deflection at any point on the web center line to the maximum deflection, and the abscissa is the ratio of the distance of the point from the flange base to the total flange width at the web center line. The flanges are drawn to scales of equal area on the figure. The flange-deflection curve starts at zero slope from the built-in edge, curves sharply, and straightens at the bulb. Flanges having relatively large bulbs tend to have s-shaped deflection curves of the web center line.

The effect of flange length on the shape of the transverse deflection curve is shown in figure 6, using flange 4 as an example. A range of flange lengths from $L/\sqrt{A_F} = 9.45$ to 27.01 was considered, since it covers the range of lengths near the minimum buckling stress value as shown by figure 3. The web center line tends to be s-shaped for low values of $L/\sqrt{A_F}$, indicating that the effective stiffness of the bulb increases rapidly with decreasing flange length.

EULER INSTABILITY OF SHEET-STRINGER STRUCTURES

A method for determining the effectiveness of the flanges in preventing instability by Euler column buckling parallel to the plane of the flange was outlined in reference 1. It was concluded that, if the structure was not to have Euler column instability before a

stress σ_{cr_s}, the largest area of sheet A_s which a flange of moment of inertia I_F about its base would stabilize was given by

$$\frac{A_s}{A_F} = \frac{\pi^2 I_F}{A_F^2\left(\frac{\sigma_{cr_s}}{E}\right)\left(\frac{L}{\sqrt{A_F}}\right)^2} - 1 \qquad (10)$$

The most efficient flange for a given stress ratio σ_{cr_s}/E and length ratio $L/\sqrt{A_F}$ will be that having the highest value of A_s/A_F. Equation (10) shows that this corresponds to having the largest value of I_F/A_F^2, that is, radius of gyration relative to the base of the flange for a given cross-sectional area. This conclusion assumes that no other instability occurs before column failure. It rules out flanges with large values of I_F/A_F^2 which fail by any other instability at relatively low stress. Inspection of column (14) of table 1 shows that flange 4 has the highest value of I_F/A_F^2 and is closely followed by flanges 9, 6, 5, and 10. Inspection of figure 3 shows that, of this group of five flanges, flange 4 also has the highest local buckling strength σ_{cr}/E for all values of $L/\sqrt{A_F}$ and that this strength is well into the plastic range since it is never less than 0.0147. Flange 4, therefore, is the best of the 10 flanges considered in this report.

The area of sheet A_s, which flanges having the shape of flange 4 can support, is shown in figure 7 for a range of values of σ_{cr_s} (the Euler column instability stress of the structure) from $\sigma_{cr_s}/E = 0.004$ to 0.015. The ordinate in this figure is A_s/A_F while the abscissa is $L/\sqrt{A_F}$. The area of sheet A_s which can be stabilized decreases sharply as either σ_{cr_s}/E or $L/\sqrt{A_F}$ increases. At high stress, $\sigma_{cr}/E = 0.012$, and reasonable length, $L/\sqrt{A_F} = 40$, A_s is slightly less than twice A_F.

COMPARISON OF PRESENT FLANGES WITH SIMPLY SUPPORTED FLANGES

It is of interest to compare the performance of the present flanges clamped at the root with the performance given in reference 1 for similar flanges simply supported at the root.

In reference 1 it was found that the most effective flanges had relatively compact cross sections. The best over-all flange width ranged from $1.9\sqrt{A_F}$ to $2.6\sqrt{A_F}$ and bulb width from $0.7\sqrt{A_F}$ to $1.2\sqrt{A_F}$. In the present report the best flange has a somewhat slimmer appearance, with a flange width of $3.4\sqrt{A_F}$ and a bulb width of $1.2\sqrt{A_F}$.

National Bureau of Standards
Washington, D. C., October 17, 1947

APPENDIX

SOLUTION BY INTEGRATION METHOD

A solution for the buckling strength of a plate built in at one edge and restrained by an elastic beam at the opposite edge may be obtained as follows:

The equation of the plate surface is (reference 5, p. 324)

$$\frac{\partial^4 w}{\partial x^4} + 2\frac{\partial^4 w}{\partial x^2 \partial y^2} + \frac{\partial^4 w}{\partial y^4} = -\frac{\sigma_{xt}}{D}\frac{\partial^2 w}{\partial x^2} \tag{A1}$$

At the edge $y = b$ (reference 5, p. 343)

$$D\left(\frac{\partial^2 w}{\partial y^2} + \nu\frac{\partial^2 w}{\partial x^2}\right) = GJ_T \frac{\partial^3 w}{\partial x^2 \partial y} \tag{A2}$$

for torsional edge condition, and at the edge $y = b$ (reference 5, p. 346)

$$EI\frac{\partial^4 w}{\partial x^4} = D\left[\frac{\partial^3 w}{\partial y^3} + (2 - \nu)\frac{\partial^3 w}{\partial x^2 \partial y}\right] - A_b\sigma_x \frac{\partial^2 w}{\partial x^2} \tag{A3}$$

for lateral-force edge condition. At the edge $y = 0$ (reference 5, p. 344)

$$\left.\begin{aligned} w &= 0 \\ \frac{\partial w}{\partial y} &= 0 \end{aligned}\right\} \tag{A4}$$

Following pages 341 and 337 of reference 5 and taking $m = 1$,

$$w = \sin\frac{\pi x}{L}\left[A(\cos \beta y - \cosh \alpha y) + B\left(\sin \beta y - \frac{\beta}{\alpha}\sinh \alpha y\right)\right] \tag{A5}$$

where

$$\alpha = \sqrt{\frac{\pi^2}{L^2} + \sqrt{\frac{\sigma_x t \pi^2}{DL^2}}}$$

$$\beta = \sqrt{-\frac{\pi^2}{L^2} + \sqrt{\frac{\sigma_x t \pi^2}{DL^2}}}$$

and A and B must satisfy the conditions of equations (A2) and (A3). These give two simultaneous equations for A and B which will only have nonzero values for a particular value of σ_x.

The two conditional equations, with expressions for the partial derivatives obtained from equation (A5) substituted, $\left(-\sin \frac{\pi x}{L}\right)$ factored out, and y set equal to b, are:

$$D\left[A\left(\beta^2 \cos \beta b + \alpha^2 \cosh \alpha b + \frac{\nu\pi^2}{L^2} \cos \beta b - \frac{\nu\pi^2}{L^2} \cosh \alpha b\right) + B\left(\beta^2 \sin \beta b + \alpha\beta \sinh \alpha b + \frac{\nu\pi^2}{L^2} \sin \beta b - \frac{\nu\pi^2\beta}{\alpha L^2} \sinh \alpha b\right)\right] =$$

$$GJ_T\left[A\left(-\frac{\pi^2\beta}{L^2} \sin \beta b - \frac{\pi^2\alpha}{L^2} \sinh \alpha b\right) + B\left(\frac{\pi^2\beta}{L^2} \cos \beta b - \frac{\pi^2\beta}{L^2} \cosh \alpha b\right)\right] \tag{A6a}$$

and

$$\left(-EI\frac{\pi^4}{L^4} + A_b\sigma_x \frac{\pi^2}{L^2}\right)\left[A(\cos \beta b - \cosh \alpha b) + B\left(\sin \beta b - \frac{\beta}{\alpha} \sinh \alpha b\right)\right] =$$

$$D\left[A\left(-\beta^3 \sin \beta b + \alpha^3 \sinh \alpha b\right) + B\left(\beta^3 \cos \beta b + \alpha^2\beta \cosh \alpha b\right) + (2 - \nu)A_b \frac{\pi^2}{L^2}(-\beta \sin \beta b - \alpha \sinh \alpha b) + (2 - \nu)B\frac{\pi^2}{L^2}(\beta \cos \beta b - \beta \cosh \alpha b)\right] \tag{A6b}$$

Solving equations (A6a) and (A6b) for A/B gives

$$A/B = \frac{GJ_T \frac{\pi^2\beta}{L^2}(\cos \beta b - \cosh \alpha b) - D\left(\beta^2 \sin \beta b + \alpha b \sinh \alpha b + \frac{\nu\pi^2}{L^2} \sin \beta b - \frac{\nu\pi^2\beta}{\alpha L^2} \sinh \alpha b\right)}{GJ_T \frac{\pi^2}{L^2}(\beta \sin \beta b + \alpha \sinh \alpha b) + D\left(\beta^2 \cos \beta b + \alpha^2 \cosh \alpha b + \frac{\nu\pi^2}{L^2} \cos \beta b - \frac{\nu\pi^2}{L^2} \cosh \alpha b\right)} \tag{A7a}$$

and

$$A/B = \frac{D\beta\left[\left(\beta^2 \cos \beta b + \alpha^2 \cosh \alpha b\right) + (2-\nu)\frac{\pi^2}{L^2}(\cos \beta b - \cosh \alpha b)\right] - \left(-EI\frac{\pi^4}{L^4} + A_b\sigma_x \frac{\pi^2}{L^2}\right)\left(\sin \beta b - \frac{\beta}{\alpha} \sinh \alpha b\right)}{D\left[\beta^3 \sin \beta b - \alpha^3 \sinh \alpha b + (2-\nu)\frac{\pi^2}{L^2}(\beta \sin \beta b + \alpha \sinh \alpha b)\right] + \left(-EI\frac{\pi^4}{L^4} + A_b\sigma_x \frac{\pi^2}{L^2}\right)(\cos \beta b - \cosh \alpha b)} \tag{A7b}$$

For a given flange geometry the quantities A_b, b, L, J_T, I_b, D/E, and t are known. The value of ν is taken as 0.3.

For a given value of σ_x/E there can be computed

$$\alpha b = \sqrt{\pi^2 \frac{b^2}{L^2} + \sqrt{\frac{\sigma_x}{E} \pi^2 (10.92) \frac{b^4}{t^2 L^2}}} = r$$

$$\beta b = \sqrt{-\pi^2 \frac{b^2}{L^2} + \sqrt{\frac{\sigma_x}{E} \pi^2 (10.92) \frac{b^4}{t^2 L^2}}} = s$$

$$\frac{GJ_T \pi^2}{L^2} \frac{1}{Eb^2} = \frac{J_T \pi^2}{2.6 b^4} \frac{b^2}{L^2} = j$$

$$b^2/L^2 = c$$

$$D \frac{1}{Eb^3} = \frac{t^3}{10.92 b^3} = h$$

$$\left(-EI \frac{\pi^4}{L^4} + A_b \sigma_x \frac{\pi^2}{L^2}\right) \frac{1}{E} = -\pi^4 \frac{I}{L^4} + \pi^2 \frac{A_b}{L^2} \frac{\sigma_x}{E} = p$$

Let

$$U = \frac{js(\cos s - \cosh r) - h\left[s^2 \sin s + rs \sinh r + 2.961c\left(\sin s - \frac{s}{r} \sinh r\right)\right]}{j(s \sin s + r \sinh r) + h\left[s^2 \cos s + r^2 \cosh r + 2.961c(\cos s - \cosh r)\right]}$$

$$V = \frac{hs\left[s^2 \cos s + r^2 \cosh r + 16.78c(\cos s - \cosh r)\right] - p\left(\sin s - \frac{s}{r} \sinh r\right)}{h\left[s^3 \sin s - r^3 \sinh r + 16.78c(s \sin s + r \sinh r)\right] + p(\cos s - \cosh r)}$$

The intersection of U and V plotted as functions of σ_x/E defines σ_{cr}/E.

REFERENCES

1. Goodman, Stanley, and Boyd, Evelyn: Instability of Outstanding Flanges Simply Supported at One Edge and Reinforced by Bulbs at Other Edge. NACA TN 1433, 1947.

2. Goodier, J. N.: Torsional and Flexural Buckling of Bars of Thin-Walled Open Section under Compressive and Bending Loads. Jour. Appl. Mech., vol. 9, no. 3, Sept. 1942, pp. A-103 - A-107.

3. Kappus, Robert: Drillknicken zentrisch gedrückter Stäbe mit offenem Profil im elastischen Bereich. Luftfahrtforschung, Bd. 14, Lfg. 9, Sept. 20, 1937, pp. 444-457. Also NACA TM 851, 1938.

4. Lundquist, Eugene E., and Fligg, Claude M.: A Theory for Primary Failure of Straight Centrally Loaded Columns. NACA Rep. 582, 1937.

5. Timoshenko, S.: Theory of Elastic Stability. First ed., McGraw-Hill Book Co., Inc., 1936.

6. Kroll, W. D.: Tables of Stiffness and Carry-Over Factor for Flat Rectangular Plates under Compression. NACA ARR 3K27, 1943.

7. Lundquist, Eugene E., Stowell, Elbridge Z., and Schuette, Evan H.: Principles of Moment Distribution Applied to Stability of Structures Composed of Bars or Plates. NACA Rep. 809, 1945.

8. Windenburg, Dwight F.: The Elastic Stability of Tee Stiffeners. Proc. Fifth Int. Cong. Appl. Mech. (Sept. 12th - 16th, 1938, Cambridge, Mass.), John Wiley & Sons, Inc., 1939, pp. 54-61.

9. Chwalla, E.: Das allgemeine Stabilitätsproblem der gedrückten, durch Randwinkel verstärkten Platte. Ing.-Archiv, Bd. V, Heft 1, Feb. 1934, pp. 54-65.

TABLE 1.- PROPERTIES AND DIMENSIONS OF REINFORCED FLANGES ANALYZED

(a) Reinforcing bulbs of rectangular shape

(1)	(2)	(3)	(4)	(5)	(6)	(7)	(8)	(9)	(10)	(11)	(12)	(13)	(14)
Flange	Corresponding flange in reference 1	t (in.)	b/t	b_1/t_1	b/b_1	$I_{b_{(in.^4)}}$	J_T $(in.^4)$	A_b $(in.^2)$	A_F $(in.^2)$	D/E $(in.^3)$	$\frac{\sigma_{cr_{min}}}{E}$	I_F $(in.^4)$	I_F/A_F^2
1	3	0.12	15	2	2	0.09505	0.022869	0.426728	0.642728	0.15824×10^{-3}	0.184	1.586931	3.8415
2	13	.24	5	4	3	.002015	.000846	.041073	.329073	1.26593	.0567	.197776	1.8264
3	14	.12	10	4	3	.001986	.000211	.041073	.185073	.15824	.0235	.128296	3.7456
4	15	.08	15	4	3	.001980	.000166	.041073	.137073	.046886	.0147	.105136	5.5956
5	27	.08	15	6	4	.0004282	.000022	.015267	.111267	.046886	.0116	.068083	5.4993

(b) Reinforcing bulbs of circular shape

(1)	(2)	(3)	(4)	(5)	(6)	(7)	(8)	(9)	(10)	(11)	(12)	(13)	(14)
Flange	Corresponding flange in reference 1	t (in.)	b/t	R_2/t	R_1/R_2	$I_{b_{(in.^4)}}$	J_T $(in.^4)$	A_b $(in.^2)$	A_F $(in.^2)$	D/E $(in.^3)$	$\frac{\sigma_{cr_{min}}}{E}$	I_F $(in.^4)$	I_F/A_F^2
6	33	0.20	15	1.0	1.0	0.002475	0.002308	0.097473	0.697473	0.73260×10^{-3}	0.00610	2.689905	5.5294
7	43	.20	5	1.5	1.5	.018111	.012297	.262736	.462736	.73260	.0640	.331342	1.5474
8	44	.20	10	1.5	1.5	.018103	.012297	.262736	.662736	.73260	.0187	1.579334	3.5958
9	45	.20	15	1.5	1.5	.018106	.012297	.262736	.862736	.73260	.0088	4.152804	5.5794
10	51	.20	15	2.0	1.0	.066148	.039617	.483707	1.083707	.73260	.0113	6.133235	5.2223

TABLE 2.- BUCKLING STRESS-RATIO VALUES OBTAINED BY BOTH STRAIN-ENERGY METHOD AND INTEGRATION METHOD

Flange	$L/\sqrt{A_F}$	σ_{cr}/E	
		Obtained by strain-energy method	Obtained by integration method
1	12.47	0.0244	0.0244
	19.96	.0185	.0184
2	5.23	.0570	.0570
	17.43	.2207	.2207
3	11.62	.0236	.0236
4	18.91	.0147	.0147
5	5.40	.0233	.0233
	29.98	.0245	.0245
6	7.18	.00648	.00648
	8.98	.00614	.00614
7	5.88	.0666	.0666
	7.35	.0642	.0642
8	4.91	.0333	.0333
	9.83	.0187	.0187
9	12.92	.00880	.00880
10	5.76	.0270	.0270
	14.41	.0113	.0113

NACA

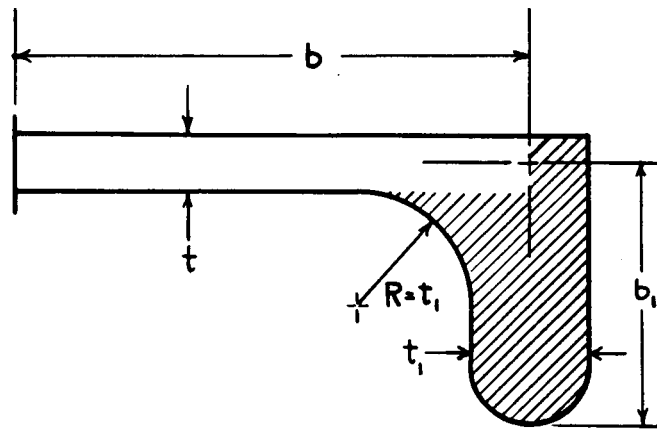

(a) Rectangular-type bulb.

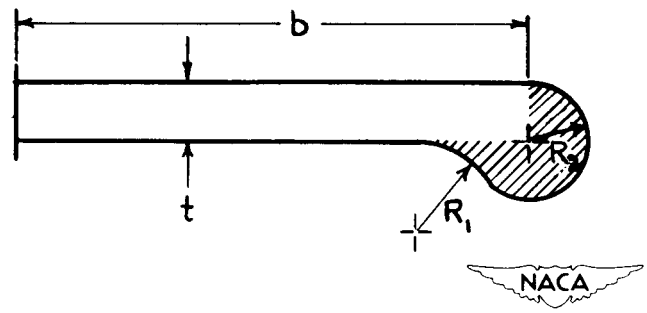

(b) Circular-type bulb.

Figure 1.- Shapes of reinforced flanges.

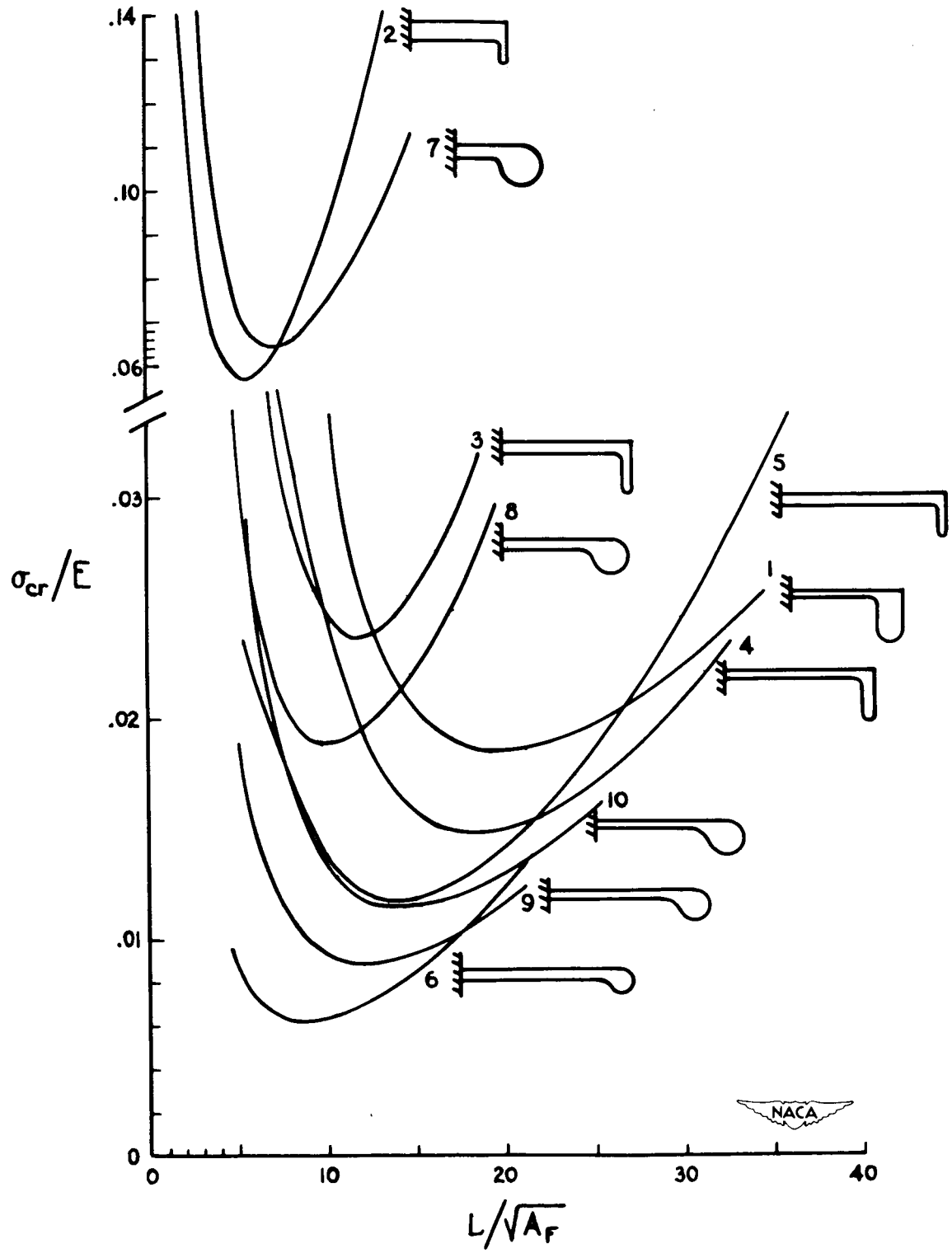

Figure 2.- Elastic buckling strength of flanges.

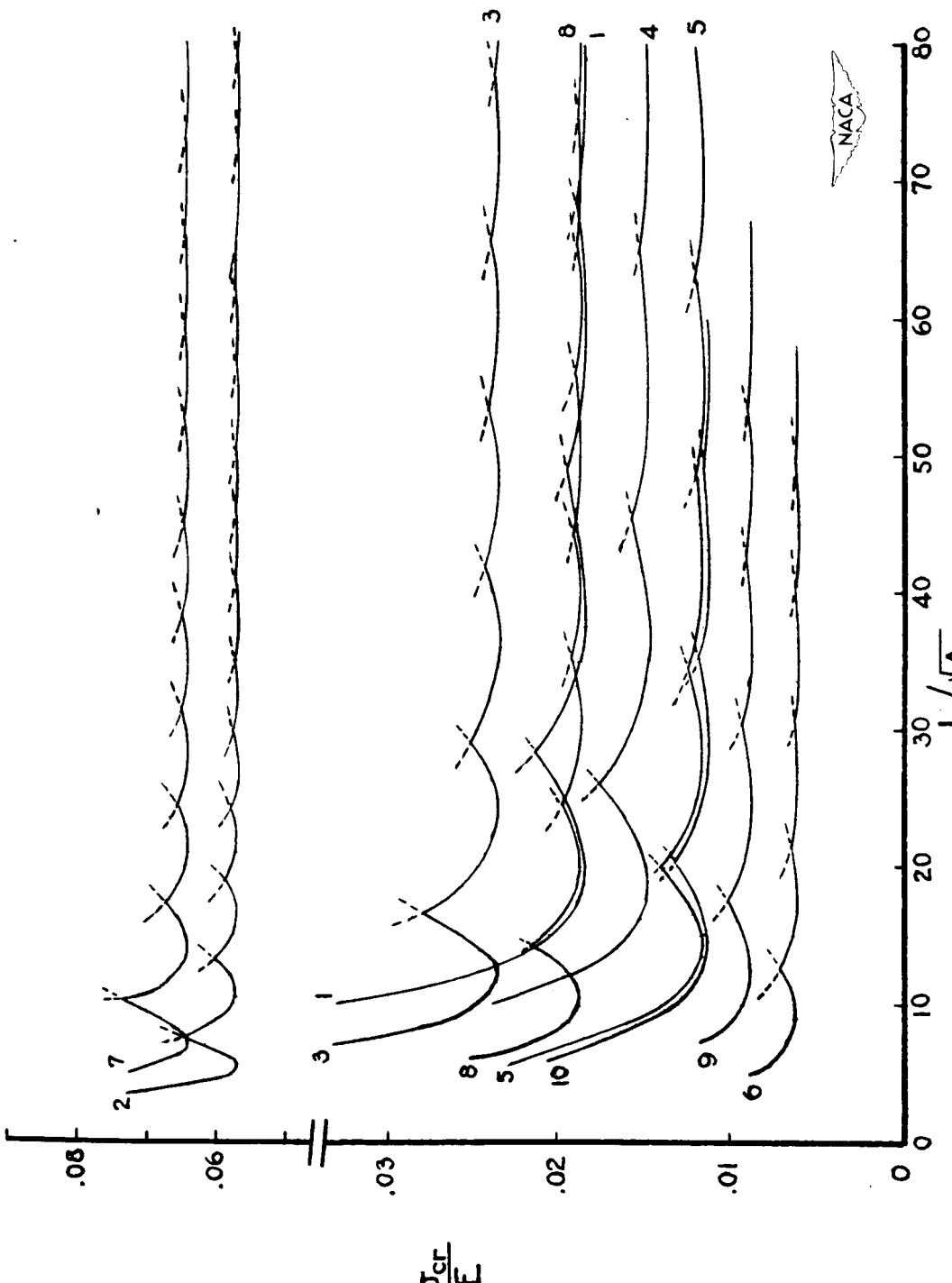

Figure 3.- Critical stress of flanges buckling in one or more half waves.

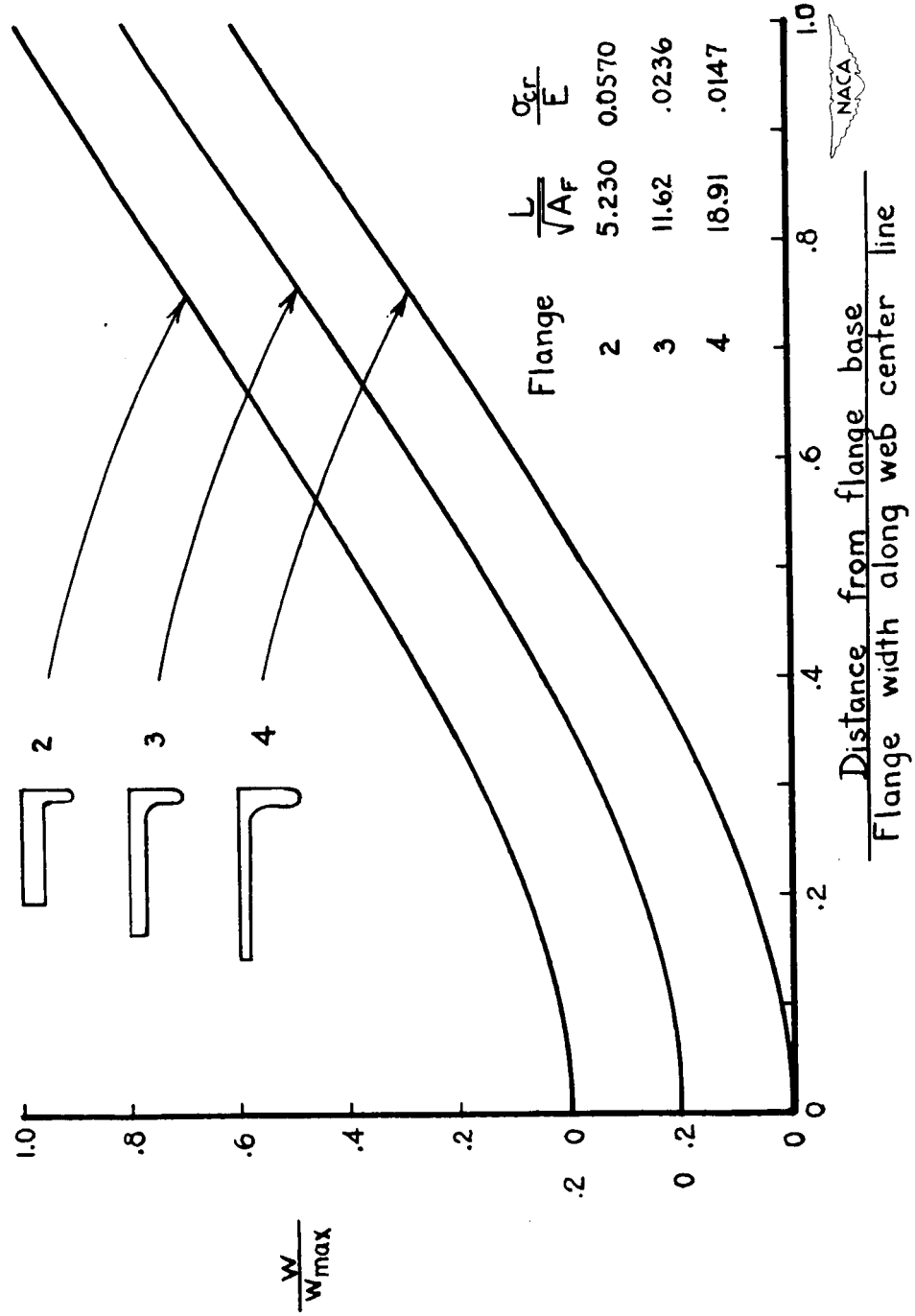

Figure 4.- Amplitude of transverse deflection of web center line for rectangular-type bulb flanges subjected to buckling stress.

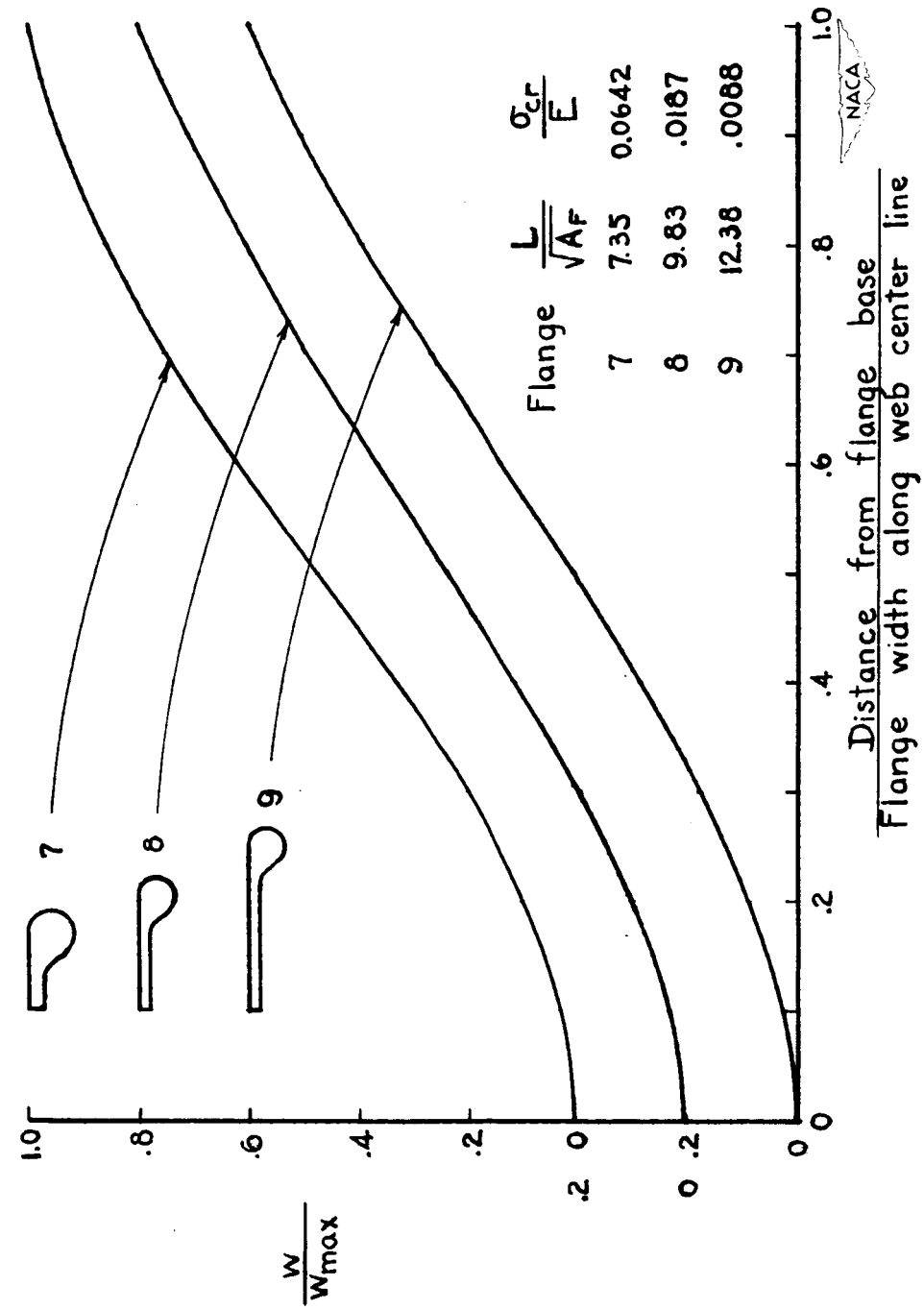

Figure 5.- Amplitude of transverse deflection of web center line for circular-type bulb flanges subjected to buckling stress.

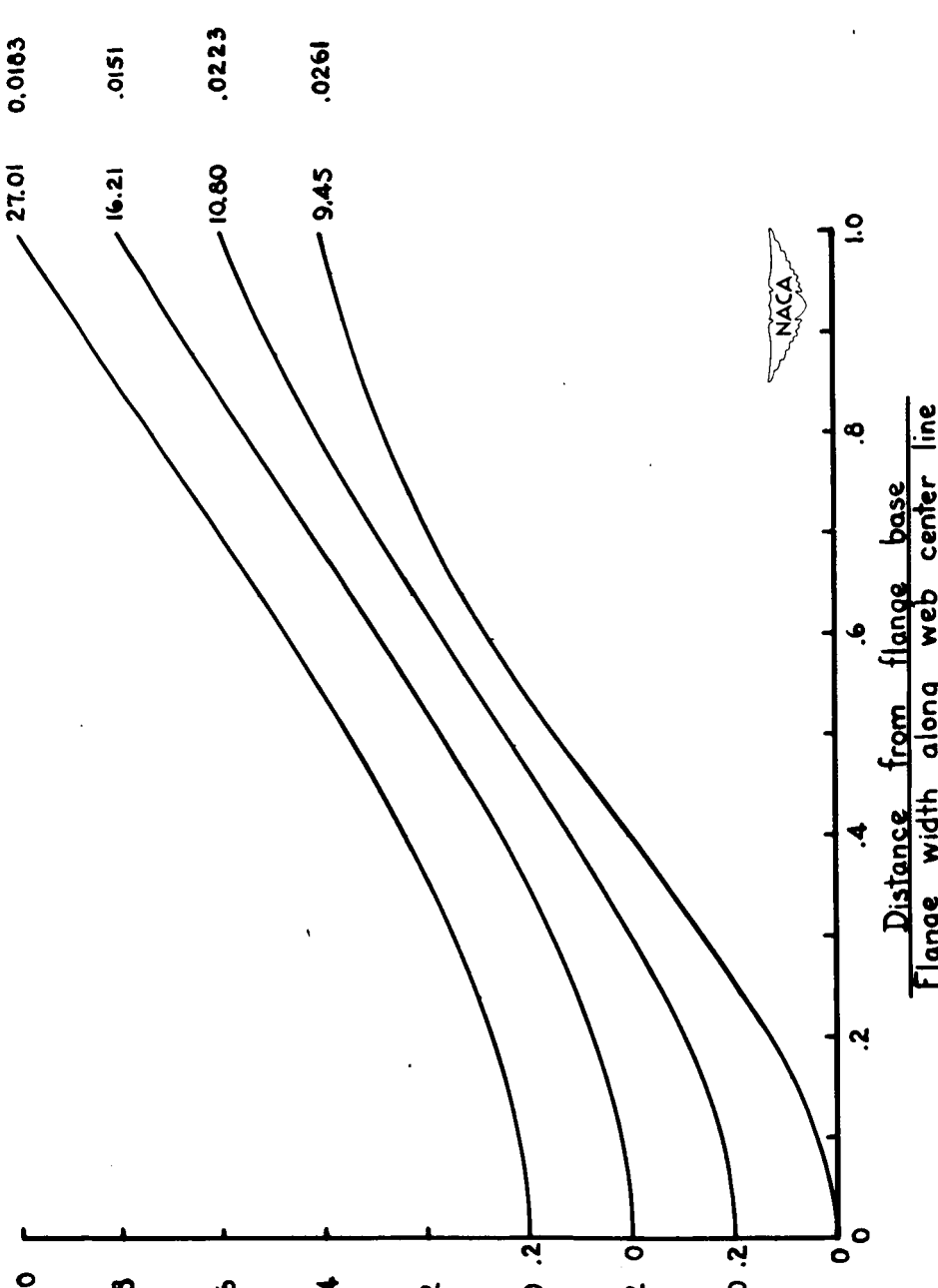

Figure 6.- Amplitude of transverse deflections at web center line for flange 4 at buckling stress.

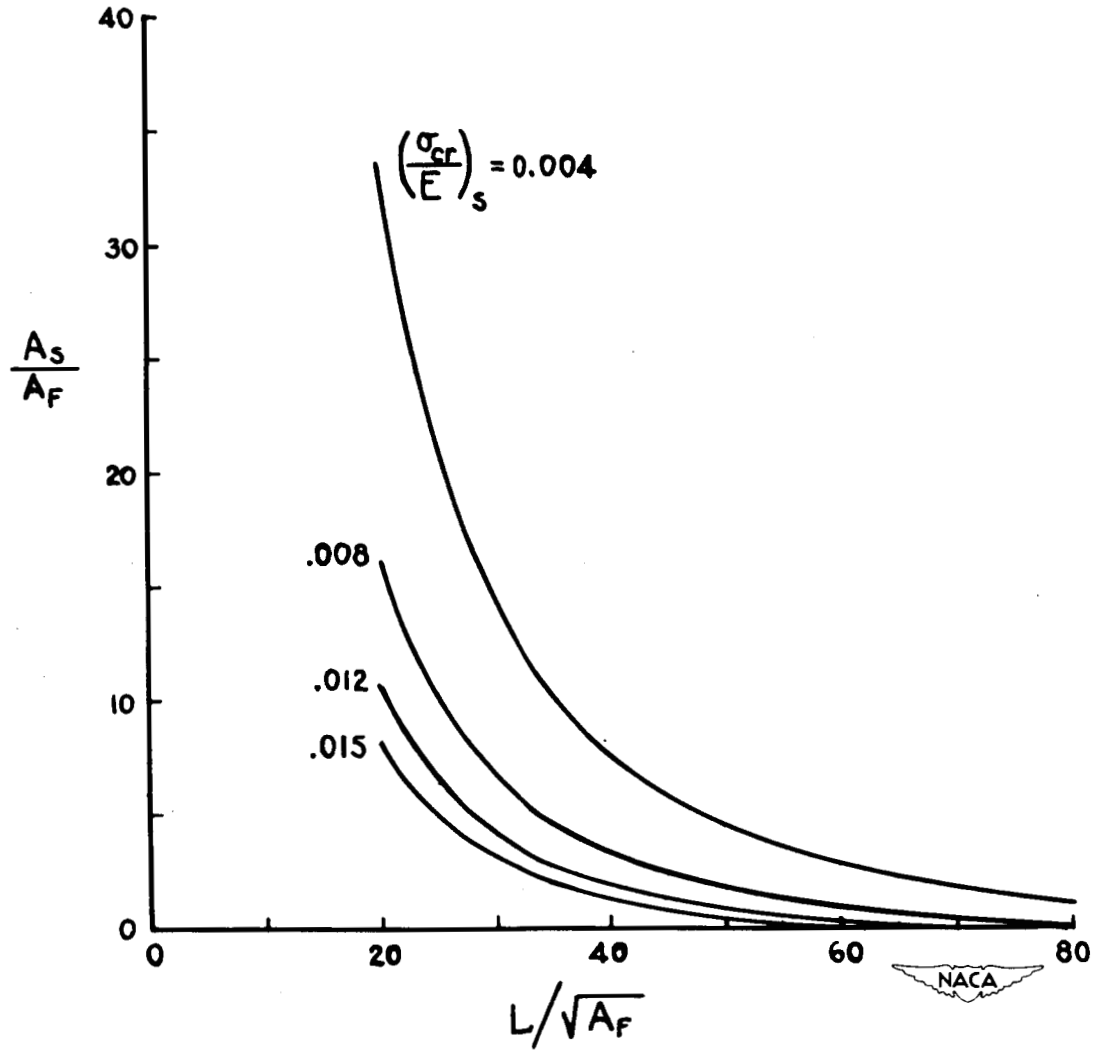

Figure 7.- Area of sheet capable of stabilization by flange 4.